Supplementary information

Sputtered binder-free Cu_3N electrode materials for high-performance quasi-solid-state asymmetric supercapacitor

Zhengbing Qi,[a,c] Binbin Wei,*[a,c] Hao Shen,[b] Zhuo Hou,[a] Minjie Fang,[a] JinGang Wu,[a] Hanfeng Liang,*[b] and Zhoucheng Wang*[b]

[a] *Key Laboratory of Functional Materials and Applications of Fujian Province, School of Materials Science and Engineering, Xiamen University of Technology, Xiamen 361024, China*

[b] *College of Chemistry and Chemical Engineering, Xiamen University, Xiamen 361005, China*

[c] *These authors contributed equally*

*Corresponding author: bbwei@xmut.edu.cn (B.B. Wei), hfliang@xmu.edu.cn (H.F. Liang) and zcwang@xmu.edu.cn (Z.C. Wang)

Specific capacity:

The areal capacity of all thin film electrodes and asymmetric supercapacitor (ASCs) can be calculated from GCD curves according to the following equation:[1]

$$C_a = \frac{2I\int Udt}{SU\Big|_{U_1}^{U_2}} = \frac{2I\int Udt}{S(U_2\text{-}U_1)}$$

where C_a (mC cm^{-2}) represents the areal capacity, I (mA) is the discharge current, $\int Udt$ is the integral area, S (cm^2) is the geometrical area of single electrode or ASC device, and U (V) is the potential with initial and final values of U_1 and U_2.

Charge balance:

The optimal areal ratio between positive and negative electrode was altered according to the charge balance denoted in equation:

$$\frac{S_{(Cu_3N)}}{S_{(AC)}} = \frac{C_{(AC)} \times \Delta U_{(AC)}}{C_{(Cu_3N)} \times \Delta U_{(Cu_3N)}}$$

Where S, C and ΔU are the area, specific capacitance and voltage range for positive and negative electrodes.

Energy and power densities:

The energy and power densities of ASCs device are calculated through the following formulas:

$$E = \frac{I\int Udt}{3.6 \times S}$$

$$P = \frac{3.6 \times E}{t}$$

where E (μWh cm^{-2}) is the energy density, P (mW cm^{-2}) is the power density, and t is the discharge time.

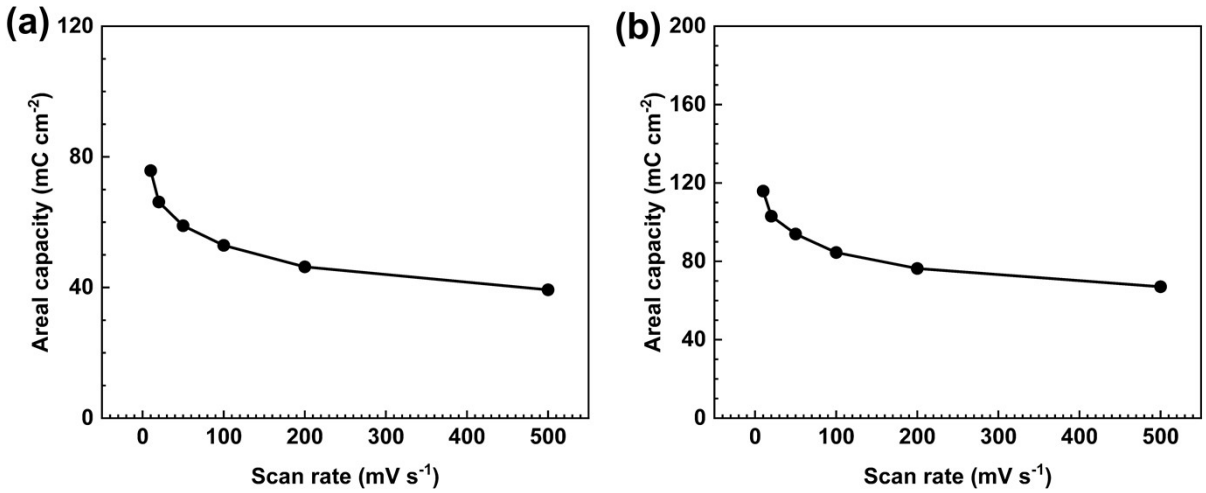

Fig. S1 Areal capacity of (a) Cu_3N thin film electrodes and (b) Cu_3N//AC quasi-solid-state ASCs with respect to scan rate.

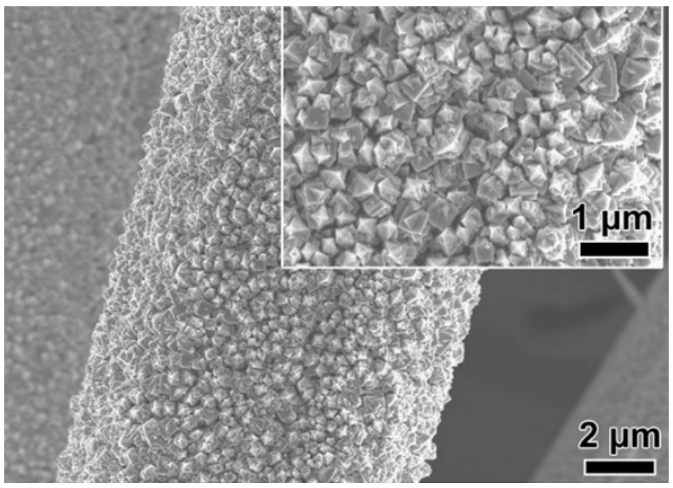

Fig. S2 SEM images of Cu_3N thin film electrodes after 20000 cycles.

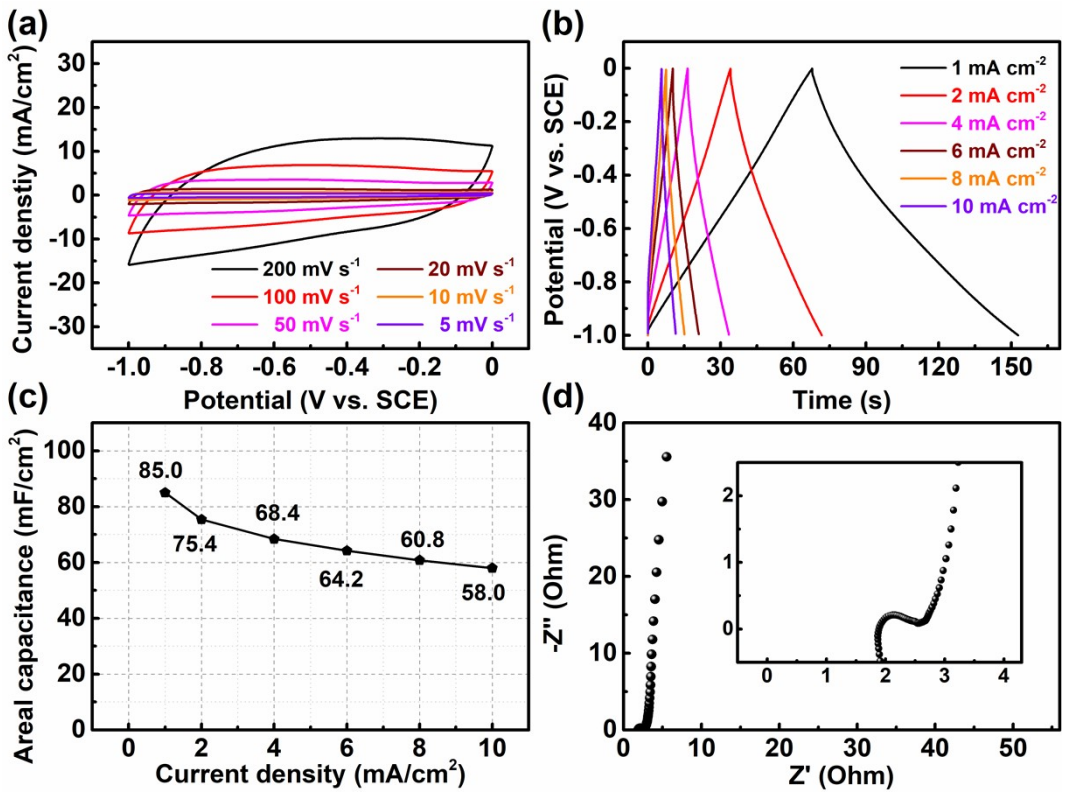

Fig. S3 Electrochemical properties of AC negative electrodes: (a) CV profiles at different scan rates, (b) GCD curves at different current densities, (c) Areal capacitance as the function of current density, and (d) Nyquist plot (inset: the enlarged part in high-frequency region).

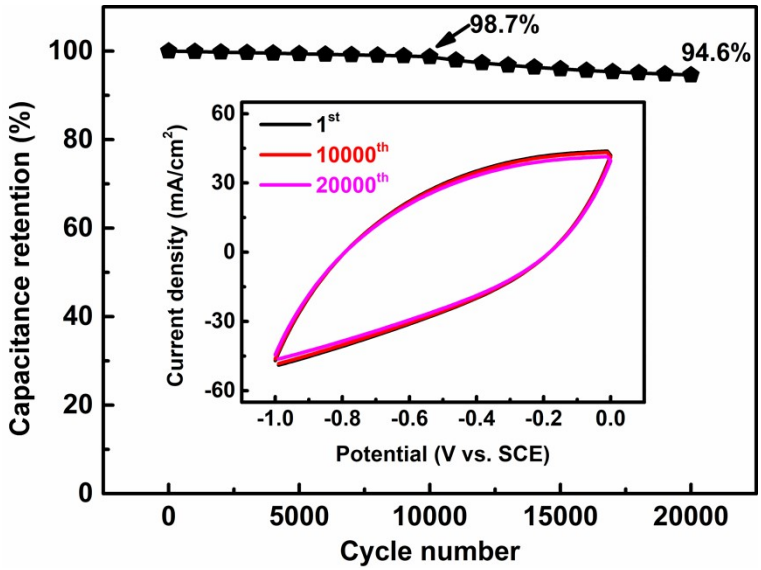

Fig. S4 Cycling performance of AC negative electrodes (inset shows the 1st, 10000th and 20000th CV curves).

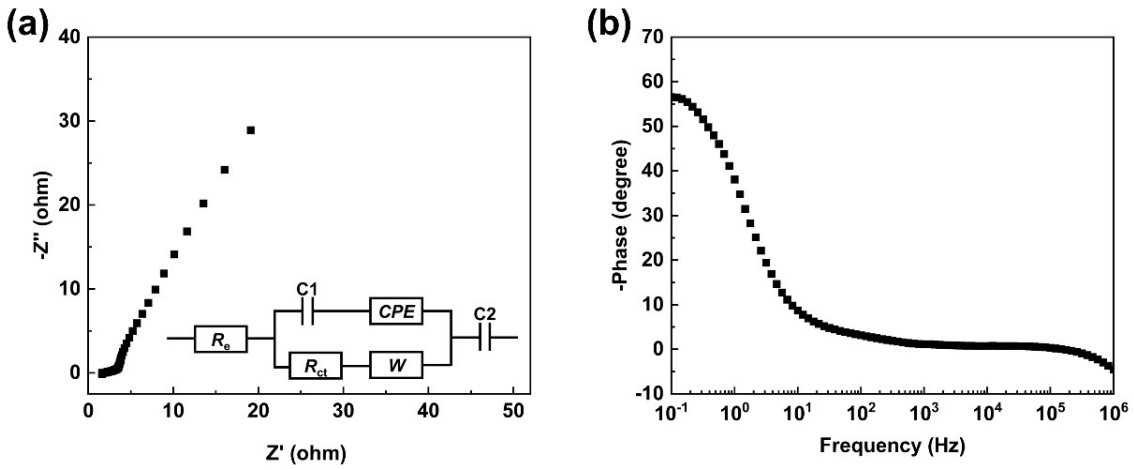

Fig. S5 (a) Nyquist (inset: the corresponding electrical equivalent circuit) and (b) Bode plots of Cu_3N//AC quasi-solid-state ASCs.

Table S1 Sample identification and deposition parameters of all thin films by magnetron sputtering

Parameter settings	CN-280	CN-320	CN-360	CN-400
Deposition pressure (Pa)	2.0	2.0	2.0	2.0
$N_2/(N_2+Ar)$	40%	40%	40%	40%
Substrate temperature (°C)	280	320	360	400
Deposition time (min)	30	30	30	30
Power (W)	250	250	250	250

Table S2 Overview of TMNs electrodes for supercapacitor applications

Electrode materials	Electrolyte	Specific capacity （capacitance）	Potential Window	References
		90.7 mC cm^{-2} at1 mA cm^{-2}		
Cu_3N film	KOH	151.1 mF cm^{-2} at1 mA cm^{-2}	0.6 V	This work
		88.2 mF cm^{-2} at 100 mV s^{-1}		
TiNbN film	H_2SO_4	59.3 mF cm^{-2} at 1.0 mA cm^{-2}	0.8 V	[1]
VN film	H_2SO_4	103.2 mF cm^{-2} at 100 mV s^{-1}	0.35 V	[2]
TiN nanoparticles	H_2SO_4	68.9 mF cm^{-2} at 1.0 mA cm^{-2}	0.8 V	[3]
CrN film	H_2SO_4	31.9 mF cm^{-2} at 100 mV s^{-1}	0.8 V	[4]
CrN film	H_2SO_4	31.3 mF cm^{-2} at 1.0 mA cm^{-2}	0.8 V	[5]
γ-Mo_2N film	Li_2SO_4	52.4 mF cm^{-2} at 10 mV s^{-1}	0.8 V	[6]
CrN@NCs@CP	H_2SO_4	132.1 mF cm^{-2} at 1.0 mA cm^{-2}	0.8 V	[7]
CrN film	H_2SO_4	40.6 mF cm^{-2} at 1.0 mA cm^{-2}	0.8 V	[8]
VN film	KOH	40.8 mF cm^{-2} at 100 mV s^{-1}	1.4 V	[9]
Mn_3N_2	KOH	115 mF cm^{-2} at 1.0 mA cm^{-2}	0.9 V	[10]
W_2N	KOH	75.0 mF cm^{-2} at 100 mV s^{-1}	1.4 V	[11]
TiN	KCl	43.5 mF cm^{-2} at 100 mV s^{-1}	1.0 V	[12]
CrVN	KCl	37.7 mF cm^{-2} at 100 mV s^{-1}	1.0 V	[13]

Table S3 Performance comparison with reported TMNs supercapacitor

Electrode materials	Electrolyte	Energy density ($\mu Wh\ cm^{-2}$)	Power density ($mW\ cm^{-2}$)	References
Cu_3N//AC	KOH	13.2	4.8	This work
VN//VN	KOH	4.6	1.5	[2]
H-TiN NPs//H-TiN NPs	H_2SO_4/PVA	2.65	0.4	[3]
CrN@NCs@CP//CrN@NCs@CP	H_2SO_4	5.28	1.98	[7]
CrN//CrN	H_2SO_4	2	8.7	[8]
VN//VN	KOH	0.3	2.4	[9]
VN//VN	KOH	3.4	3.3	[14]
VN//VN	KOH	10.0	4.0	[14]
VN/CC//VN/CC	PVA/KOH	0.11	15	[15]
VN/V_2O_3/C// VN/V_2O_3/C	KOH	4	0.48	[16]

References

[1] B. B. Wei, F. W. Ming, H. F. Liang, Z. B. Qi, W. S. Hu and Z .C. Wang, *J. Power Sources* 2021, **481**, 228842.

[2] B. Asbani, K. Robert, P. Roussel, T. Brouse and C. Lethien, *Energy Storage Mater.* 2021, **37**, 207-214.

[3] P. Qin, X. X. Li, B. Gao, J. J. Fu, L. Xia, X. M. Zhang, K .F. Huo, W. L. Shen and P. K. Chu, *Nanoscale* 2018, **10**, 8728-8734.

[4] J. Shi, B. L. Jiang, Z. Liu, C. Li, F. Y. Yan, X. S. Liu, H. T. Li, C. Yang and D. Dong, *Ceram. Int.* 2021, **47**, 18540-18549.

[5] B. B. Wei, G. Mei, H. F. Liang, Z. B. Qi, D. F. Zhang, H. Shen and Z. C. Wang, *J. Power Sources* 2018, **385**, 39-44.

[6] L. M. Chen, C. Liu and Z. J. Zhang, *Electrochim. Acta* 2017, **245**, 237-248.

[7] X. Xu, S. Y. Chang, Z. Z. Hong, Y. Zeng, H. Zhang, P. Li, S. Z. Zheng, Z. C. Wang and S. W. Duo, *Nanotechnology* 2021, **33**, 055402.

[8] E. Haye, A. Achour, A. Guerra, F. Moulaï, T. Hadjersi, R. Boukherroub, A. Panepinto, T. Brousse, J. -J. Pireaux and S. Lucas, *Electrochim. Acta* 2019, **324**, 134890.

[9] K. Robert, C. Douard, A. Demortière, F. Blanchard, P. Roussel, T. Brousse and C. Lethien, *Adv. Mater. Technol.* 2018, **3**, 1800036.

[10] G. Durai, P. Kuppusami, T. Maiyalagan, M. Ahila and P. V. Kumar, *Ceram. Int.* 2019, **45**, 17120-17127.

[11] S. Ouendi, K. Robert, D. Stiévenard, T. Brousse, P. Roussel and C. Lethien, *Energy Storage Mater.* 2019, **20**, 243-252.

[12] N. N. Sun, D. Y. Zhou, W. W. Liu, S. Y. Shi, Z. J. Tian, F. Liu, S. D. Li, J. J. Wang and F. Z. Ali, *ACS Sustainable Chem. Eng.* 2020, **8**, 7869-7878.

[13] D. Durai, K. Kuppusami, T. Maiyalagan, J. Theerthagiri, V. K. Ponnusamy and H. -S. Kim, *Ceram.*

Int. 2019, **45**, 12643-12653.

[14] K. Robert, D. Stiévenard, D. Deresmes, C. Douard, A. Iadecola, D. Troadec, P. Simon, N. Nuns, M. Marinova, M. Huvé, P. Roussel, T. Brousse and C. Lethien, *Energy Environ. Sci.* 2020, **13**, 949-957.

[15] Z. Q. Wu, H. Li, H. Li, B. B. Yang, R. H. Wei, X. G. Zhu, X. B. Zhu and Y. P. Sun, *Chem. Eng. J.* 2022, **444**, 136597.

[16] Y.F. Zhang, X.F. Wang, J.Q. Zheng, T. Hu, X. Liu and C.G. Meng, *Appl. Surf. Sci.* 2019, **471**, 842-851.